Nanostructured Superhydrophobic Substrates Trigger the Development of 3D Neuronal Networks

*Tania Limongi, Fabrizia Cesca, Francesco Gentile, Roberto Marotta, Roberta Ruffilli, Andrea Barberis, Marco Dal Maschio, Enrica Maria Petrini, Stefania Santoriello, Fabio Benfenati, and Enzo Di Fabrizio**

The generation of 3D networks of primary neurons is a big challenge in neuroscience. Here, a novel method is presented for a 3D neuronal culture on superhydrophobic (SH) substrates. How nano-patterned SH devices stimulate neurons to build 3D networks is investigated. Scanning electron microscopy and confocal imaging show that soon after plating neurites adhere to the nanopatterned pillar sidewalls and they are subsequently pulled between pillars in a suspended position. These neurons display an enhanced survival rate compared to standard cultures and develop mature networks with physiological excitability. These findings underline the importance of using nanostructured SH surfaces for directing 3D neuronal growth, as well as for the design of biomaterials for neuronal regeneration.

1. Introduction

Most of the cellular processes such as growth, adhesion, migration, secretion, and death are influenced by the 3D organization of the cell-substrate interface. Cells respond to local concentrations of a large number of molecules that are dissolved in the extracellular medium, present on the underlying surface (extracellular matrix) or exposed on the membrane of adjacent cells. In 3D cell cultures, the interactions between cells and substrate are controlled by space constraints, i.e., geometry and topology, and by the chemical and physical properties of the substrate. It is well known that cell behavior can be adjusted through changes in micro- and nanoscale topographic features, and that the control of wettability may also have an important role in the behavior of biocompatible substrates.[1]

Imposing specific geometries to the surface of a biocompatible solid device and changing its wetting behavior and/or surface–volume ratio makes the design closely related to the molecular/cellular scale. Hence, wettability and roughness were found to be two of the most important factors influencing cells biological reactions at biomaterial surfaces.[2–5] It is known that cell spreading, alignment and migration are influenced by the geometry and the dimensions of the surface features.[6] One of the models that account for this is the 'contact guide effect', according to which integrins, present in focal contacts, transfer the variable degree of tension or compression to the cytoskeleton, which will reorganize itself based on the surface topography.[7–9] As a consequence, cell adhesion and spreading are often observed to be delayed and less pronounced on hydrophobic materials.[10]

Dr. T. Limongi,[+] Dr. F. Gentile, S. Santoriello, Prof. E. Di Fabrizio[++]
Department of Nanostructures
Istituto Italiano di Tecnologia
Via Morego 30 - 16163 Genova, Italy
E-mail: enzo.difabrizio@iit.it
Dr. T. Limongi, Dr. F. Cesca,[+] Dr A. Barberis, Dr. M. Dal Maschio, Dr. E. M. Petrini, Prof. F. Benfenati[++]
Department of Neuroscience and Brain Technologies
Istituto Italiano di Tecnologia
Via Morego 30 - 16163 Genova, Italy
Dr. R. Marotta, R. Ruffilli
Department of Nanochemistry
Istituto Italiano di Tecnologia
Via Morego 30 - 16163 Genova, Italy
Dr. F. Gentile
Department of Experimental and Clinical Medicine
BioNEM Laboratory
University Magna Grecia of Catanzaro
Viale Europa- 88100 Catanzaro, Italy
[+] These authors share first authorship.
[++] These authors share last authorship.

DOI: 10.1002/smll.201201377

small NANO MICRO

In this respect, the growth, development and differentiation of neurons is particularly interesting.[11] Indeed, one of the major topics in neuroscience research is to reproduce in vitro the complexity of the 3D connections characterizing brain neural networks. A large body of experimental evidence demonstrates that neurons can grow and form functional connections in vitro, and that these processes are conditioned by structural cues given by the substrate as well as chemical cues present in the surrounding environment. While substrate topography can affect the directional growth of neuronal processes and the extent of surface adhesion by physical confinement, immobilized chemical cues are very powerful to attract or inhibit process growth, as well as to recognize the correct targets for establishing synaptic connections.[12–14] Two-dimensional cultures of primary neurons, although useful to study the molecular mechanisms modulating neuronal growth and survival, represent an oversimplification of the brain structure. 3D neuronal cultures are therefore essential for reproducing the complexity of directional growth and connections, to resemble more closely the in vivo situation.

The ability of neurons to respond to topographical features has been reported in the literature.[9,15,16] Previous studies have shown how neurons[15–17] and astrocytes[18] can be cultured on microgrooved platforms with various depths, particularly on substrates with repeating topography. It has been demonstrated that submicron grooves can support guidance of neurites of rat hippocampal neurons,[16] in a manner dependent on the surface features. Neurites undergoing this guidance extended perpendicularly to the grooves, crossing over adjacent grooves and ridges rather than extending along the major groove axis. In addition, neuronal and astrocytic processes were found to span grooves of a dimension larger than the cell body, by anchoring to the plateaus by tension-bearing cellular extensions, with no underlying support (cellular bridging).[19] In some cases, astrocytes[18] were grown on arrays of 1 μm-high silicon pillars, with various diameters and pitch, demonstrating that the astroglial cells were suspended and in contact with the pillar tops. Other studies observed that hippocampal neurons plated on surfaces with 1 μm tall pillars preferentially aligned to pillar geometries.[15,16]

Superhydrophobic (SH) materials reduce the water contact area on the surfaces minimizing the adsorption of biomolecules.[20–22] The protein adsorption process is determined by several variables, such as the material surface properties and the relative protein concentrations. After a fast concentration-dependent adsorption phase, the process rate decreases in relation to the number of available binding sites, becoming progressively more dependent on the protein surface affinity.[23] Hence the surface wettability, as well as the display of functional, polar and charged groups, are the key mediators of the protein-material affinity.[24] Thus, nanostructured devices with SH surfaces could have a potential application in cell engineering due to the reduced cell adhesion.[22] While the adhesion of blood cells was found to be minimized on SH surfaces,[25] certain cell types such as macrophages grow very well on hydrophobic substrates, such as Teflon.[26] In this respect, SH 3D scaffold surfaces subjecting the neuronal membrane to hydrophobic interactions have never been exploited thus far. As the chemo-mechanical forces driving cell migration result from a balance between cell-cell and cell-substrate interactions, reduction of the latter interactions by exploiting superhydrophobicity of the substrate should maximize the cell-to-cell interactions, which determine network connectivity.

Here, we describe and validate a new and effective method of 3D growth of neurons and astrocytes using nanostructured superhydrophobic (NSH) devices fabricated by lithographic and etching techniques, which exhibit a combination in the patterned length scales. In particular, the design of the pillars was in the microscale, but their sidewall had a patterning in the nanoscale, leading to a spatial modulation in the z direction. Under these conditions, neurons grew in a suspended fashion, forming a viable and functional 3D network, a behavior that was never observed with smooth pillars, in which neurons grew on the bottom surface of the devices. Our data support the use of a combination of 3D topography, superhydrophobicity and nanostructured surfaces to direct the growth of primary neurons in a suspended 3D fashion, which allows the formation of viable and functional neuronal networks, a feature which could be exploited in the development of future biocompatible devices.

2. Results

2.1. Design and Fabrication of Nanostructured Superhydrophobic Substrates

In order to promote optimal growth of neurons onto SH devices, it was necessary to test various materials and scale the device to match the typical length scale of cells. SH surfaces made of nanopatterned silicon were deposited with a 5 nm layer of a Teflon-like (C_4F_8) polymer to assure superhydrophobicity (**Figure 1**a). Cylindrical pillars of 10 μm in height and 10 μm in diameter (Figure 1a) were arranged in a hexagonal lattice with periodicity of 30 μm (Figure 1b). The sidewalls of the pillars were either smooth (Figure 1c) or nano-sculptured with a regular pattern of grooves (Figure 1d). A drop of water, positioned upon SH surfaces, assumes a quasi-spherical shape, with a contact angle at the interface between 160° and 170° (Figure 1e) that can be theoretically predicted with excellent accuracy. In the model of Cassie and Baxter,[27] the wetting behavior of the surface is described by the sole parameter *f*, that is the ratio of the solid to the total projected area. When *f* tends to zero at the interface with the substrate, the liquid mostly 'senses' air and the droplet would resemble a perfect sphere. The most useful property of these devices is their reduced friction coefficient, which makes them a suitable tool for the manipulation of biological samples. This property will be exploited to seed neurons on the device, as explained in the following paragraph.

2.2. NSH Surfaces Drive 3D Neuronal Growth

It is well known that primary neurons require polycationic substrates, such as poly-lysine, poly-ornithine or laminin, to

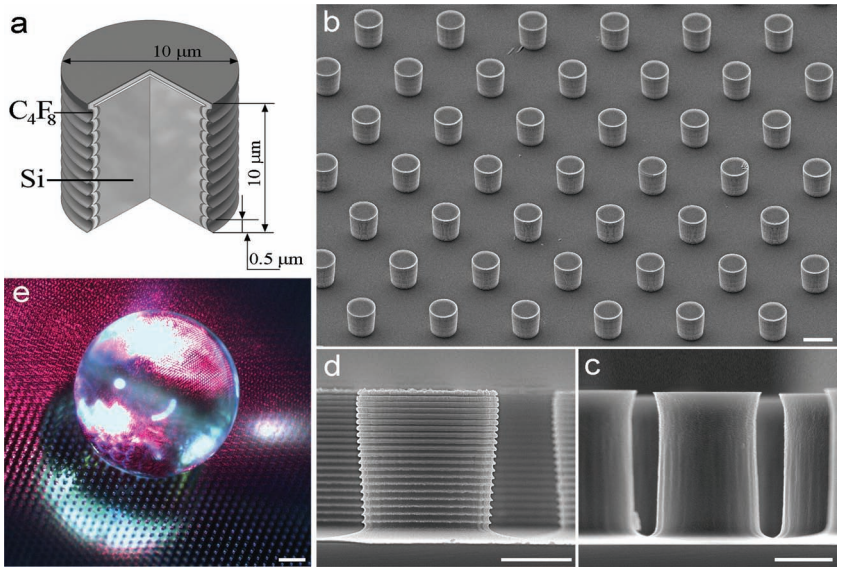

Figure 1. Construction details and high contact angle of the SH devices. (a) Compositional 3D section of a single nanopatterned pillar with technical drawings. SEM micrographs: (b) low magnification of the device surface (scale bar, 10 μm) and high magnification of the smooth (c) and nanopatterned (d) pillar sidewalls (scale bar, 5 μm). (e) Stereo microscope image of a drop that remains on the NSH surface keeping its shape and the contact angle constant.

adhere to the substrate and grow processes.[28] Therefore, we performed a standard poly-D-lysine (PDL) coating of our devices. To verify the polylysine distribution on the NSH devices, a fluorescently conjugated compound was used. Confocal imaging showed that the poly-lysine coating was mostly concentrated at the top surface and around the base of the pillars, while staining at the lateral surface was likely below the detection limit of the confocal microscope (Supporting Information (SI), Figure 1a).

Cell cultures were carried out in parallel on two different types of SH devices bearing pillars without (smooth) and with nanopatterned sidewalls, as shown in SI, Figure 1b. Hippocampal neurons were plated using two different seeding methods. Using the "volume seeding" method, 200 000 cells were plated in 3 mL of medium, which completely submerged the device. Using the "drop seeding" method, 50 000 cells were plated on the device in a 150 μL drop of medium. As mentioned above, the drop placed on the surface of the NSH device adopted a quasi-spherical shape with a contact angle greater than 160° that was preserved at the high relative humidity (95%) of the cell culture incubator, preventing evaporation and the consequent reduction of the drop volume. When the cells were seeded onto the NSH devices, they were first randomly distributed within the drop. In the following hours, cells settled and accumulated at high density in a highly localized region at the contact between the drop and the surface of the pillars. Notably, these two plating methods gave completely different results in terms of cell attachment and viability. No cells attached and survived upon "volume seeding", on both smooth and grooved pillars, while the "drop seeding" method yielded viable and healthy neuronal cultures on both NSH substrates, which we extensively characterize in the following paragraphs. Thus, the SH interactions between the drop, the cells and the pillars at the early stages after plating are crucial for the attachment and survival of the neurons on these devices.

Next we characterized by scanning electron microscopy (SEM) the in vitro development of hippocampal neurons drop-plated on either nanopatterned or smooth SH substrates to closely analyze the interaction of neurons with the micropillars (**Figure 2** and SI, Figures 2 and 3). From the very first hours of growth, neurites adhered to the plateaus of the NSH substrates and were able to pull neurons into a suspended bridge arrangement. Devices with nanopatterned sidewall were able to spatially control and direct neurite growth and promote the formation of suspended bridges composed of both cell bodies and processes, which extended between adjacent pillars, forming a dense 3D network (Figure 2a,b and SI, Figure 2a,b,g,h). The neuronal projections, singularly or more often organized in large bundles, overran on the top of the pillars and densely wrapped the grooved surfaces (Figure 2a,c). Small filopodial processes transversally connected the neurites within each bundle. Close to the pillars, neurites extensively branched and intertwined thin processes that tightly anchored inside the pillar's threads (Figure 2a,c; SI, Figure 2c–f). Numerous lamellipodial and filopodial-like extensions, few hundred nanometers thick, emerged from single neuritic tips, to spread on the nanopatterned surface (Figure 2c and SI, Figure 2f).

On the contrary, neurons and their projections laid at the base of the pillars on smooth sidewall SH substrates, forming a flat sparse neuronal network (Figure 2d–e). The neuritic projections were fewer and stouter compared to those present on NSH substrates. Moreover, they were attached only to the basal portion of the smooth pillar sidewalls, without reaching their apical surfaces (Figure 2e,f and SI, Figure 3). Altogether, these data demonstrate that the high affinity of the neurons for the 'rough' pillars compared to the smooth pillars is directly dependent on their nanostructure. In further support to our SEM data, 3D reconstruction of confocal images also shows that grooved pillars support the 3D growth of the network (SI, Movie 1). As 3D/suspended growth was observed only on the grooved pillars, we further characterized the functional properties on neuronal cultures only on these substrates.

2.3. SH Substrates Allow Optimal Viability and Proper Differentiation of Neurons

We performed a viability assay on primary hippocampal cultures grown on standard polystyrene culture dishes and on NSH devices, at different days in vitro (DIV) (**Figure 3**). Neurons grown in standard 2D culture dishes were characterized by a high mortality (around 50%) at early stages after

small NANO MICRO

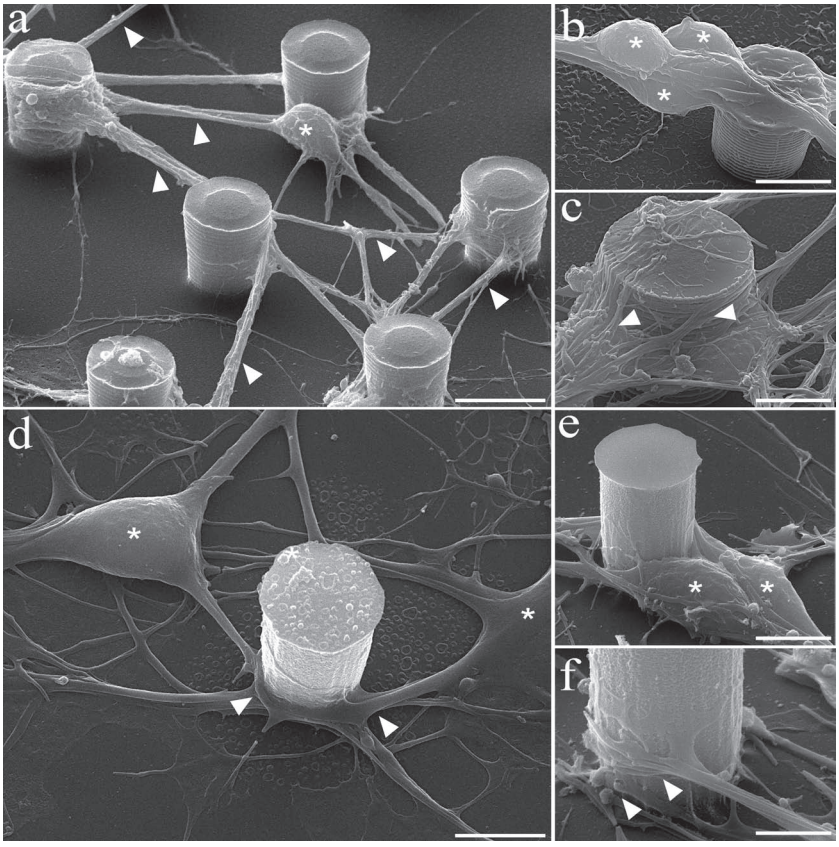

Figure 2. Scanning electron micrographs of 3 DIV hippocampal neurons drop-plated on superhydrophobic nanostructured (a–c) and smooth (d–f) pillared substrates. (a) Low magnification: both the neuronal somas (asterisk) and their processes, often organized in bundles (arrowheads), are suspended between adjacent nanostructured pillars. (b) Higher magnification of a small group of suspended neuronal cell bodies (asterisks) close to a pillar. (c) Neuronal projections from 3 DIV neurons densely wrap the pillar nanopatterned sidewall (arrowheads). (d) Low magnification of neuronal cell bodies (asterisks) and their processes (arrowheads) lying at the base of the smooth pillars. (e) A small group of neuronal cell bodies (asterisks) at the base of a pillar. (f) High magnification of neuronal processes attached to the base and the lower part of a smooth pillar (arrowheads). Scale bars: 10 μm (a,d), 5 μm (b,c,e), and 3 μm (f).

plating, which decreased with time. On the contrary, neurons grown on 3D devices showed a significantly lower mortality rate at early times after plating, which is the most critical step for neuronal survival and development.

To better characterize the growth and development of cultures plated on NSH devices, as well as the correct localization and distribution of neuron-specific proteins required for proper neuronal excitability and synaptic transmission, we performed an immunocytochemical analysis by using an array of antibodies (**Figure 4**). We visualized the expression of adhesion molecules (neuronal cell adhesion molecule, NCAM; Figure 4a,a'), the organization of the actin and tubulin cytoskeleton (Figure 4b,c), the expression and distribution of markers of axonal differentiation (axonal marker SMI-31 and Na^+-channels; Figure 4d,e) as well as the formation of excitatory (vGlut-positive) and inhibitory (vGAT-positive) synapses by using the synaptic vesicle markers synapsin I, vGlut1/2 and vGAT (Figure 4f,g). The expression and localization of all these markers were compatible with a physiological growth and differentiation of NSH-plated neurons, in terms of neuritic development, synapse formation, neurotransmitter release machinery and correct molecular equipment for generation/propagation of electrical signals. The distribution of such markers is comparable to what is observed in standard 2D neuronal cultures (SI, Figure 4). Interestingly, NCAM was highly concentrated in the neuronal domains contacting the top of the pillars (Figure 4a,a', arrowheads), indicating the strong adhesion of neurons to these structures.

Taken together, these results indicate that the geometry of the devices, which was chosen to provide stable hydrophobic conditions, can promote excellent survival, growth and differentiation of primary hippocampal neurons. In addition, it allowed neurons to contact several adjacent pillars, effectively forming a 3D network.

2.4. Neurons Grown onto NSH Substrates Display Normal Excitability, Firing, and Synaptic Transmission

To test the functional properties of neurons growing on NSH substrate, electrical activity was measured and compared to that of control neurons growing in standard culture dishes. In a first set of experiments performed in current clamp mode, we studied the neuronal firing activity induced by depolarization of the neuronal membrane (see Experimental Section). The mean frequency of action potentials triggered by the injection of 0.5 nA was not significantly different under control conditions and in neurons grown on NSH devices (31.5 ± 3.4 and 34.2 ± 5.6 Hz, for control and NSH substrate neurons, respectively). The action potential firing threshold was 38.8 ± 0.7 and 38.9 ± 1.2 mV in control and NSH substrate-growing neurons, respectively (**Figure 5**a,b). Then, we investigated the spontaneous synaptic currents of both excitatory (glutamatergic) and inhibitory (GABAergic) synapses. To this purpose, whole-cell recordings were performed in voltage-clamp mode in the presence of bicuculline or kynurenic acid to isolate spontaneous excitatory or inhibitory postsynaptic currents (sEPSCs or sIPSCs), respectively. As shown in Figure 5c,e both sEPSCs and sIPSCs recorded under the two experimental conditions did not show any difference in the mean frequency, peak amplitude, and decay kinetics of postsynaptic currents (Figure 5d,f).

In order to further confirm the normal membrane properties of neurons grown on NSH substrates, Ca^{2+} imaging was performed on test cultures at DIV14. Similar patterns

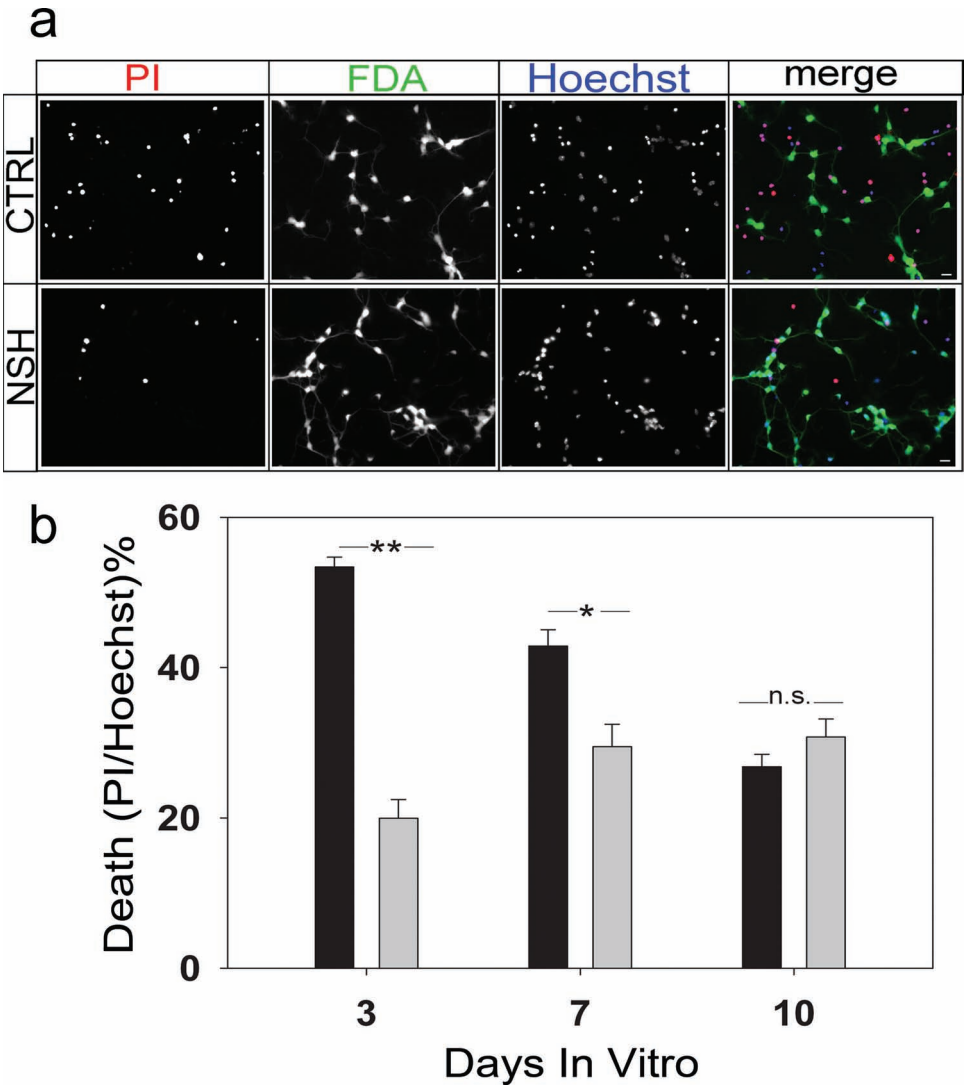

Figure 3. NSH substrates promote optimal survival of cultured neurons. Neurons grown on NSH devices or on standard culture dishes (CTRL) for 3, 7, and 10 DIV were incubated in extracellular medium containing PI, FDA, and Hoechst (see Experimental Section) and immediately imaged. (a) Representative images of 3 DIV neurons grown on polystyrene dishes (CTRL) or on NSH substrates. Note the higher number of PI-positive nuclei in control cultures, compared to cultures on NSH substrates. (b) The percentages of dying cells (black for control and gray for NSH devices) were calculated as the ratio of PI-positive nuclei on total (Hoechst-positive) nuclei (PI/Hoechst) and are shown as mean±standard error of the mean. Statistics were performed using the two-tailed, unpaired Student's t-test. n.s.: non significant. $n > 20$ for each condition. * $p = 0.002$; ** $p < 0.001$, $t = 12.955$ with 62 degrees of freedom. Scale bars, 20 µm.

of population spontaneous activity characterized by sparse and mostly desynchronized Ca^{2+} transients were observed throughout in both control and NSS cultures due to spontaneous firing (**Figure 5**g and SI, Movie 2).

2.5. NSH Substrates are Compatible with the Growth of Neuron-Astrocyte Co-Cultures

Our results indicate that NSH substrates can promote the survival and differentiation of healthy and functional neuronal cultures, thus laying the basis for future in vivo applications of these devices. To get a better understanding of whether such devices would be compatible with the in vivo environment, we tested the biocompatibility of NSH devices with the growth of mixed cultures of primary neurons and glial cells. Hippocampal neurons were plated on mature glial cultures (see Experimental Section for details), and the growth and differentiation of the co-cultures were assessed by both SEM and confocal microscopy. As shown in **Figure 6**, glial cells adhered with high affinity to both the top and the lateral surface of the pillars, and provided an excellent support for the survival of co-cultured neurons (Figure 6a). Glial cells expressed physiological astrocytic markers, such as GFAP (Figure 6b–d), and allowed strong adhesion of neurons, as shown by the high expression of the neuronal adhesion protein NCAM (Figure 6c–d).

small NANO MICRO

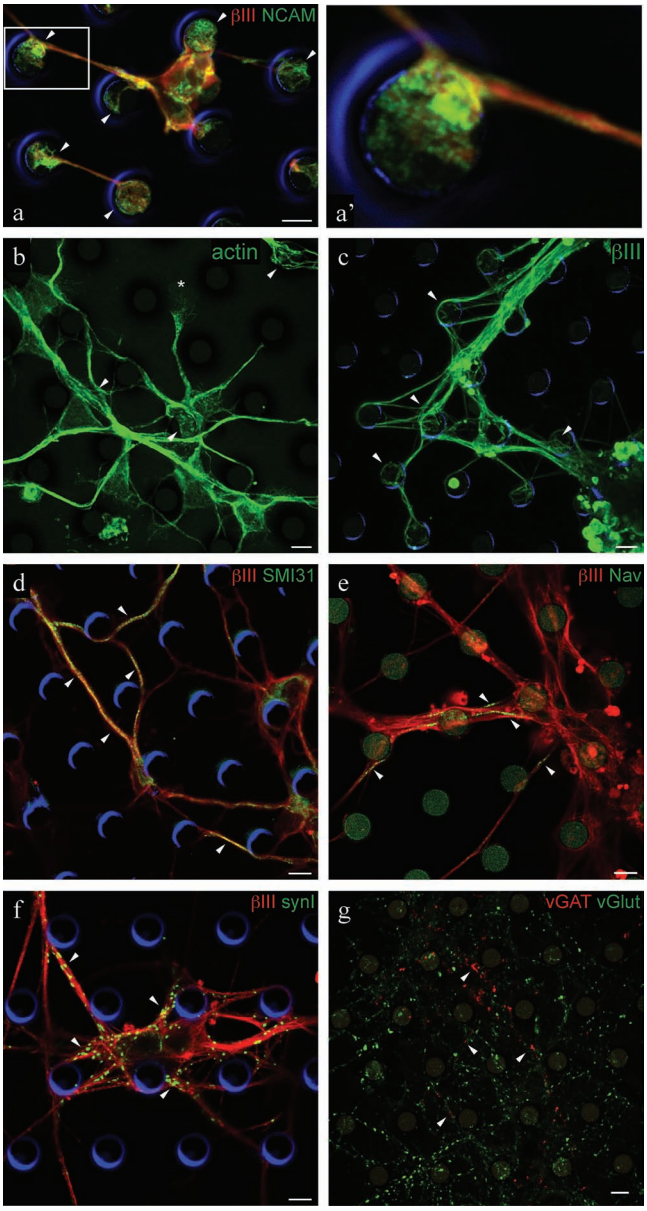

Figure 4. Immunocytochemical characterization of primary hippocampal cultures grown on NSH substrates. Neurons were grown on NSH substrates for 3 (a,a'), 7 (b,c), or 10 (d–g) DIV, fixed and stained using the indicated antibodies. (a) A strong expression of the adhesion molecule NCAM (green) is detected in the regions of contact between the neurons and the pillars (arrowheads). (a') Higher magnification of the boxed image in (a), showing the area of contact between a neurite and the pillar top. (b,c) Actin and *β*III-tubulin cytoskeleton develops around the pillars (arrowheads). The asterisk in (b) indicates a growth cone. (d,e) SMI-31 staining indicated the presence of normally developed axons (arrowheads in (d)) bearing Na^+-channels correctly localized at the axonal initial segment (arrowheads in (e)). (f,g) Cultures grown on NSH substrates develop synaptic connections labeled by the synaptic vesicle protein synapsin I (synI, arrowheads in (f)), and differentiate excitatory (vGlut-positive; green) and inhibitory (vGAT-positive, red) neurons. Arrowheads in (g) point to the synaptic terminals of inhibitory neurons. Scale bars, 10 µm. In the images where the patterned substrate was not clearly visible, the outline of the pillars was rendered in the blue channel.

3. Discussion

It is generally accepted that biomimetic scaffolds offer the most favorable prospect to culture specific cell types and investigate different aspects of cell-matrix interaction in 3D to support applications in tissue engineering, nerve regeneration and stem cell research.[1,3,9] In this paper, we describe a new 3D neuronal cell culture system, as an efficient tool for growing cells in a setting that closely mimics the in vivo environment. The development of the network in the *z* dimension fully spans the pillar height (10 µm), with neurons extending processes out of the cell body plane. This is clearly different from conventional 2D cultures in which neurites strictly develop in adhesion with the substrate. This new culture method using NSH devices represents a clear advancement over current 2D cell culture technologies. It supports neuronal growth and differentiation in an open scaffold, reducing the interactions with the substrate and maximizing the physiological processes of cell–cell adhesion and synapse formation.

As a result, neurons cultured in this 3D culture system displayed a lower mortality rate at early stages in vitro, which are the crucial steps determining neuronal survival and development. Neurons grown under these conditions arranged themselves in a suspended network that mimics the growth environment of the developing brain, and displayed an extensive neurite network and a full complement of physiological markers. In particular, they showed a full development of the actin and tubulin cytoskeleton, a correct differentiation of the axonal domain as evidenced by the distribution of the axon-specific markers SMI31 and Nav, and a correct development of synaptic connections as visualized by the punctate staining of the specific presynaptic proteins synI, vGlut and vGAT. In addition, they showed electrophysiological properties in the physiological range, including action potential mean firing rate and threshold. Moreover, the spontaneous excitatory and inhibitory synaptic activity indicates the existence of a correct balance between excitation and inhibition, a crucial parameter for network functioning. These data were corroborated by the normal spontaneous activity, with rhythmic action potential-dependent Ca^{2+} waves observed in cell grown in superhydrophobic conditions.

In the fabrication characterization of the proposed device, the microscale is responsible for the superhydrophobicity, while the nanoscale introduces the 3D topology. Our data demonstrate that the combination of these two characteristic length scales is fundamental for the docking of neuronal processes on pillars sidewalls and for the 'suspended' 3D assembly of the neuronal network. In fact, the 3D character of the culture virtually disappeared in the presence of smooth pillar sidewalls, with neurons growing in a 2D fashion on the bed of the device. While in the very early stages in vitro neurons should find the top of pillars identical, when the processes grow and first come in contact with the pillar sides neurons are likely to make stronger contacts with grooved pillars than with smooth pillars, which are able to keep the cell bodies in a suspended 3D network. On the other hand, the weaker adhesion of cell processes to the smooth pillars

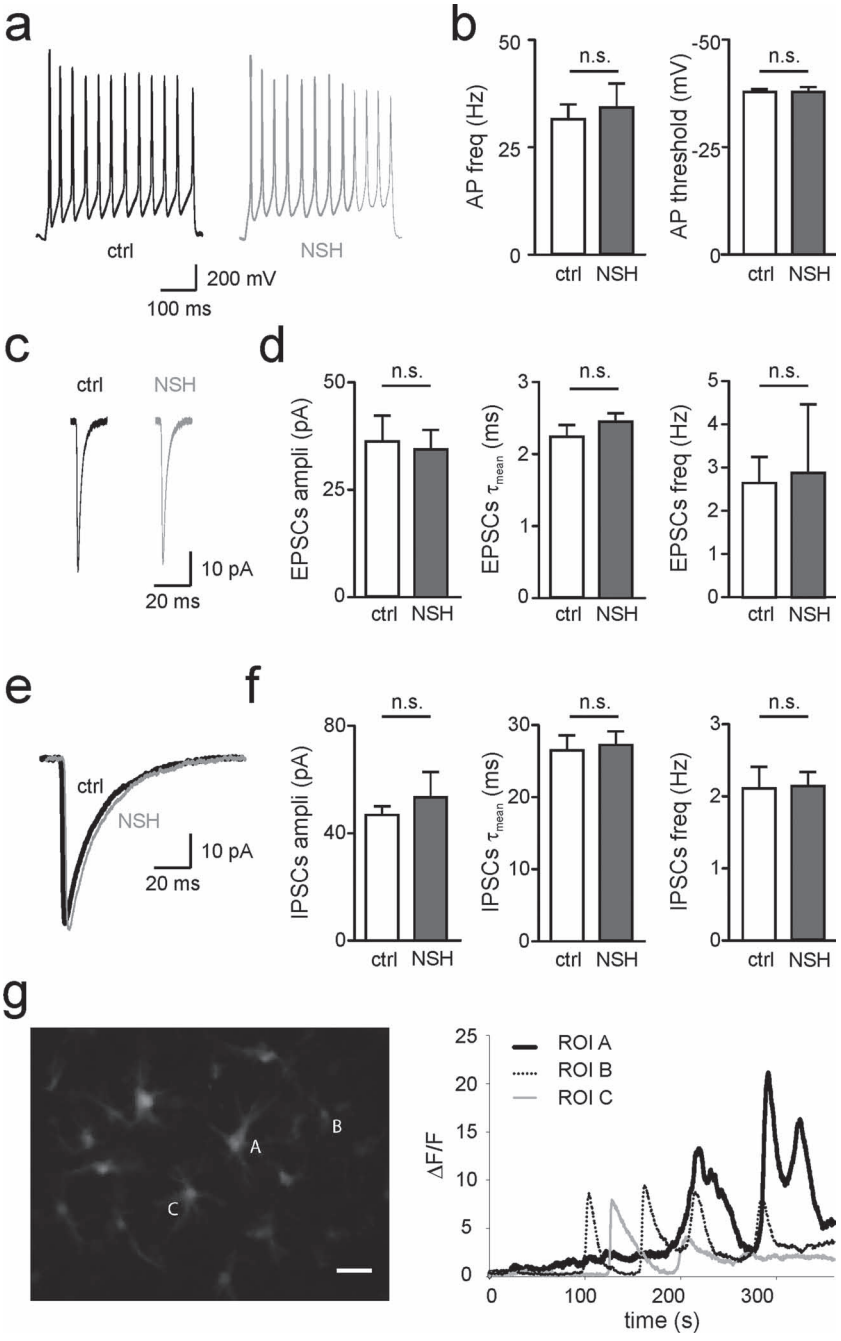

Figure 5. Neurons grown on NSH substrates exhibit normal excitability and synaptic activity. (a) Example current-clamp traces of neuronal firing upon membrane depolarization in neurons growing on control (black) and NSH substrates (grey). (b) Mean firing rate (AP freq., Hz) and threshold of action potential firing (AP threshold, mV) in the indicated conditions. (c) Representative traces of sEPSCs recorded in control and in neurons on NSH substrates. (d) Neurons grown on NSH devices exhibit sEPSC amplitude, frequency and decay time constant (t_{mean}) comparable to control. (e) Representative inhibitory synaptic currents from neurons grown on control or NSH substrates. Note that in the overlay, currents have been slightly shifted for clarity. (f) The kinetic properties of sIPSCs recorded from neurons grown on NSS are comparable to those recorded in control neurons. Data are shown as means ± SEM. Statistics was performed using the two-tailed, unpaired Student's t-test. n.s.: non significant. n > 8 for each condition. (g) Neurons cultured on NSS were loaded with Fluo4-AM and imaged. Snapshot of Fluo4-AM fluorescence taken at time = 200 s (left). Scale bar, 20 μm. The corresponding fluorescence changes in 3 representative neurons (bold, dotted and thin lines respectively) are plotted as $\Delta F/F_0$ in the right panel.

is not sufficient to support the formation of a 3D network, therefore originating a 2D network where neurons and processes lay at the bottom of the devices and the attachment is restricted to the lower part of the pillars. The suspended growth of neurons was the result of the development of tension originating from strong adhesion areas between neurons and the top surface of pillars, as shown by the very high and selective concentration of the adhesion molecule NCAM in these regions. Hence, this 3D culture system represents a valuable tool to support the long-term growth and maintenance of neuronal cells. Compared to fibrous matrices, our rigid 3D open scaffold possesses adequate stability to support neuronal growth and maturation facing the mechanical forces that are typically experienced at the scaffold-cell interface. In porous artificial matrices, proper pore interconnectivity and controlled pore size are required to accommodate cells and guide their growth in three dimensions. The design of our microfabricated device provides an 'open scaffold', which allows a better supply of nutrients and oxygen, prompt clearance of metabolic products and offer a large surface area to facilitate interactions with extracellular signaling molecules.

We demonstrated that a vertically aligned silicon nanopatterned device with low wettability promotes 3D neuronal growth and differentiation, obtaining neural networks more closely resembling the brain structure and which are of potential use in the development of implantable neuroprosthetic devices or in tissue regeneration therapies. The assembly of 3D neuronal networks in vitro with differentiated stem cells or genetically reprogrammed neurons[29] could be a first step towards transplantation of brain tissue in neurodegenerative diseases or brain trauma and such substrates might be used to assist neuronal regeneration by exploiting the ability of some classes of neurons to regrow after injury.[30]

4. Conclusion

This new culture method represents an exponential improvement over current 2D cell culture technologies, because it supports mixed-cell populations in varied microenvironments throughout

small NANO MICRO

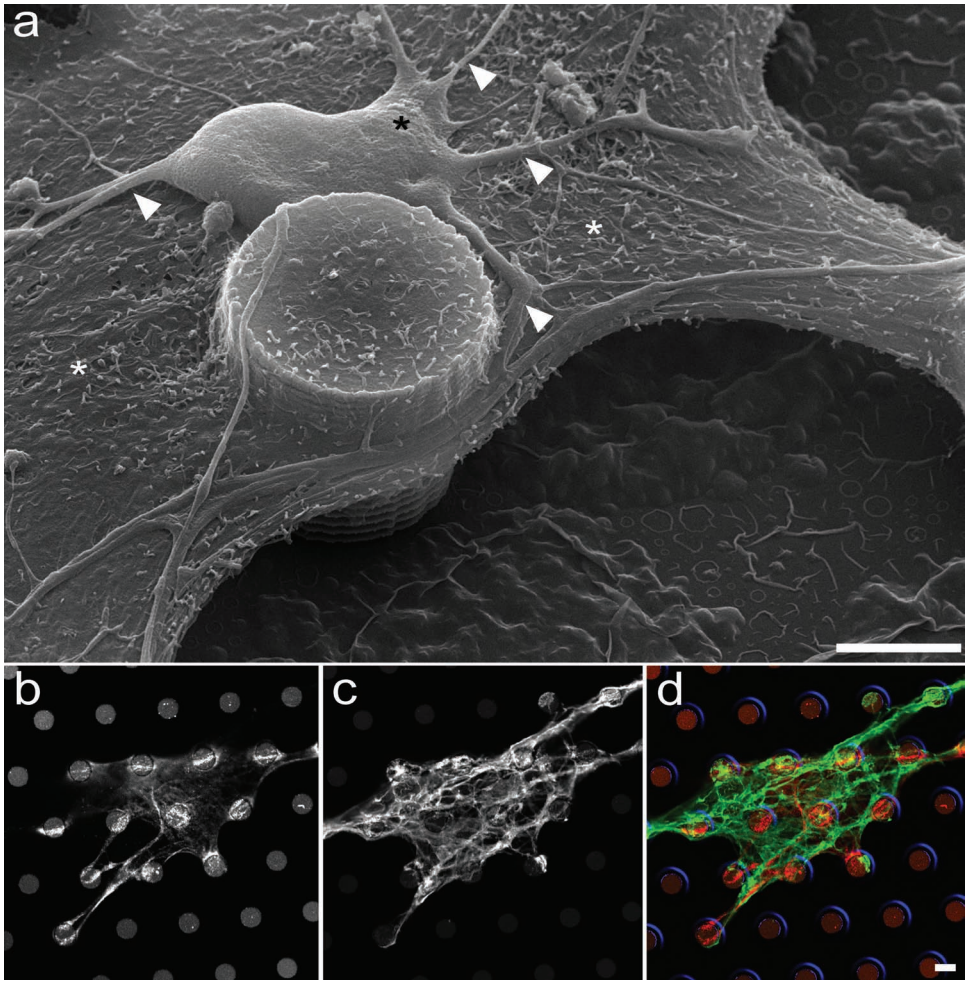

Figure 6. Neuron-glial cell co-cultures. (a) SEM micrograph showing a flat glial cell monolayer (white asterisks) suspended between adjacent nanostructured pillars. A large neuron (black asterisk) spreads upon the glial carpet with its multiple neuritic processes (arrowheads). (b–d) Co-cultures were fixed and stained for the astrocyte marker GFAP (b; red in (d)) and NCAM (c; green in (d)). Scale bars, 5 μm (a), 10 μm (b–d).

an open scaffold. Hence, this 3D culture system is proposed as a valuable tool for studying different cell types, including neuronal-glial co-cultures. Moreover, this technology has the advantage that can be scaled up for mass production because only 'parallel' processes were used during the fabrication of the devices; in other words, the unit cost of these substrates can be, in production phase, in the range few tens of euro per square centimeter. The unique nanofabricated NSH scaffold described here can be developed as a technological platform to enable routine 3D neuronal cultures, thus laying the basis for the design of future bio-compatible devices. We finally envisage that the present device can be of interest for in vitro toxicity assays, as well as to study cancer cell differentiation and migration in a 3D environment.

5. Experimental Section

Microfabrication of Nanopatterned Superhydrophobic (NSH) Surfaces: NSH surfaces were characterized by a texture of a periodic hexagonal lattice of cylindrical pillars. The diameter d and the distance l between the pillars were chosen in accordance with a criterion of optimal design as described in,[31] that is d = 10 μm and l = 20 μm; while the height of the pillars (h) was 10 μm. This way, a small fraction of solid $f = p/4\ d^2/(l+d)^2 \sim 0.09$[27] was secured, assuring an increased hydrophobicity with contact angles approaching 170°, with an f value sufficiently large to prevent the collapse of the drop at the early stage of evaporation. P-doped, (100) silicon wafers with resistivity of 5–10 Ohm/cm were used as substrates; they were cleaned with acetone and isopropanol to remove possible contaminants and then etched with a 4% hydrofluoric acid (HF) solution. The wafers were then rinsed with deionized water and dried with N_2. The masks for optical lithography were fabricated using direct laser writing (DWL66fs, HEIDELBERG Instruments). Standard optical lithography techniques (Mask Aligner, MA6/BA6, SUSS MICROTEC) were employed to generate regular patterns of disks within a layer of negative tone resist (AZ5214) that was spin-coated onto clean silicon wafers. The disks served as a mask in a Deep Reactive Ion Etching Process (DRIE) (ICP-RIE, SI 500, SENTECH Instruments GmbH), whereby the final structures were obtained in the form of cylindrical pillars with an aspect ratio greater than 2. The DRIE process utilized was a pulsed, time-multiplexed etching that alternated repeatedly between three modes, namely (i) a deposition of a chemically inert passivation

Table 1. List of parameters used in the DRIE process of nanopatterned micropillars fabrication.

	Passivation phase	Etching phase	Cleaning phase
Duration (s)	8	7	4
C4F8 gas flow (SCCM)	75	0	0
SF6 gas flow (SCCM)	0	129	30
Ar gas flow (SCCM)	0	30	10
Power at the coil (W)	1000	800	500
Power at the platen (W)	20	40	100

layer of C_4F_8; (ii) an isotropic plasma etch of SF_6; and (iii) a phase for sample/chamber cleaning. Based on this alternate process, the pillars were fabricated with a nanothreads at the sidewalls, which were characterized by indentations with a pitch depending on the duration of the isotropic plasma etch and of the passivation phase. With the passivation, etching and cleaning times being t_1, t_2 and t_3, respectively, the ratio $r = t_1/t_2$ was adjusted with high precision during process optimization to ensure vertical sidewalls. Any deviation from r would unbalance the process: if $t_1/t_2 > r$, passivation dominates over etching, the pillars would be tapered as to resemble a frustrum (truncated cone); if $t_1/t_2 < r$, etching dominates over passivation, the pillars would be shaped into an upside-down frustrum. The total time $t = t_1+t_2+t_3$ represents the total duration of a cycle. Provided that t_1/t_2 is held constant, the longer the time t, the wider is the pitch of the nanothread at the sidewalls. For the configuration used in this work, $t_1 = 8$ s, $t_2 = 7$ s, $t_3 = 4$ s and thus $t = 19$ s. This cycle yielded 500 nm thread pitch. Upon removal of the residual resist with piranha solution (H_2SO_4:H_2O_2 = 3:1 v/v), a 5 nm layer of titanium and a 100 nm layer of gold were sequentially sputtered upon the substrates. The gold layer was finally covered by a thin (5 nm) film of a Teflon-like (C_4F_8) polymer to assure superhydrophobicity. All the parameters of the process are summarized in **Table 1**.

Microfabrication of Smooth Superhydrophobic Surfaces: Superhydrophobic smooth sidewall pillars were made with the same metrology and materials used for the nanopatterned SH surfaces described above. The only difference was in the use of a positive tone resist (Megaposit SPR 220) instead of a negative tone resist; nanostructuring of the sidewalls was eliminated by using a single step deep reactive ion etching process with a controlled mixture of C_4F_8 and SF_6 (C_4F_{8flow} = 32 sccm, SF_{6flow} = 30 sccm).

Substrate Preparation: Single nanopatterned superhydrophobic substrates (1 cm^2) were placed in 35 mm tissue culture dishes, sterilized by immersion in ethanol (Fluka, Ethanol 02483; ≥99.9%), washed twice in H_2O, dried in a laminar flow hood and further sterilized by UV irradiation for 2 h. To coat the substrates, PDL (Sigma, Milan, Italy) was diluted in sterile H_2O to a final concentration of 1 μg/mL. Substrates were let float on the PDL solution overnight in a cell culture incubator (37 °C, 5% CO_2, 95% humidity) with the hydrophobic surface facing down. Before plating the cells, PDL was removed and substrates were washed in sterile H_2O and let dry.

Hippocampal Cultures: Whole brains were extracted from C57B/L6 mouse embryos at day 18 (E18). All procedures were carried out in accordance with the guidelines established by the European Communities Council (Directive of November 24th, 1986) and approved by the National Council on Health and Animal Care (authorization ID 227, prot. 4127, 25th March 2008). Pregnant females were deeply anesthetized with CO_2 and decapitated. Embryos were removed and brains were placed in cold Hank's Balanced Salts solution (HBSS). After removal of the meninges the hippocampus was carefully dissected, incubated with 0.125% trypsin for 15 min at 37 °C and mechanically dissociated. Neurons were plated on the PDL coated SH devices in Neurobasal containing 10% horse serum, 2 mM glutamine and antibiotics (plating medium). When the 'volume seeding' method was used, 200 000 neurons were plated in 3 mL of medium to completely submerge the device. In the "drop seeding" method, 50 000 cells were plated on each device, in a 150 μL drop of plating medium. The drop placed on the surface of the SH device adopted a quasi-spherical shape with a contact angle greater than 160°. The high relative humidity (95%) of the cell culture incubator prevented medium evaporation and reduction in the diameter of the drop. Neurons were plated at the same density on PDL coated plastic tissue culture dishes serving as controls. After 4 h, the plating medium was removed and replaced with Neurobasal containing 2% B27 supplement, 2 mM glutamine and antibiotics (maintenance medium). All culture media and reagents were from Invitrogen (Milano, Italy), unless otherwise specified.

Co-culture Experiments: Primary astrocytes were obtained from cortices of P0 wild-type C57B/L6 mice (with modifications from Kaech and Banker[28]). Briefly, cortices were dissected in ice-cold HBSS and incubated in 0.25% trypsin plus 1 mg/mL DNase for 30 min at 37 °C. Cells were centrifuged, resuspended in culture medium (MEM, 10% horse serum, 33 mM glucose and antibiotics) and plated onto PDL coated NSH substrates. After 24 h, the medium was replaced and cells were allowed to reach confluence in the following two weeks. Hippocampal neurons were plated onto mature glial cultures that had been starved for 48 h in maintenance medium. Co-cultures were grown for 3 to 7 days, fixed and processed for SEM or immunofluorescence.

Scanning Electron Microscopy: Cells were fixed for 1 h in a filtered (0.2 μm, Millex-LG Millipore) solution of 1.2% glutaraldehyde (G5882 Sigma) in 0.1 M cacodylate buffer (pH = 7.4) at 4 °C. After fixation, neurons were extensively washed in the same buffer, and postfixed for 1 h on ice in a filtered solution of 1% osmium tetroxide (O5500, Sigma) in cacodylate buffer 0.1 M. After several washes in ice-cold Milli-Q water, fixed samples were rinsed for 5 min in increasing concentrations of filtered ice-cold ethanol (25%, 35%, 50%, 70%, 80%, 90% and 96%), followed by 2 × 15 min rinses with ice-cold 100% ethanol. Graded dehydration with ethanol was followed by gradual replacement with ice-cold hexamethyldisilazane (52619, Sigma), that was allowed to evaporate in a fume hood overnight. Samples were then glued with silver paint (Pelco) to SEM stubs, coated with 20 nm gold/palladium in a sputter coater (108auto/SE Cressington), and observed with a JEOL JSM-6490LA variable pressure scanning electron microscope.

Immunofluorescence: The following primary antibodies were used: polyclonal anti-actin (A2066, Sigma), monoclonal and polyclonal anti-neuronal class III β-tubulin (MMS-435P, Covance, NJ and T2200, Sigma, respectively), polyclonal anti-neural cell adhesion molecule (NCAM, ab5032, Millipore, MA), monoclonal anti-phosphorylated neurofilament heavy chain (SMI-310R, Covance), monoclonal anti-pan-Na^+ channel (S8809, Sigma), polyclonal

anti-synapsin I (ab8, Abcam, UK), polyclonal anti-vesicular GABA transporter (vGAT, AB5062P, Millipore), polyclonal anti-vesicular glutamate transporter-1 (vGlut1, AB5905 Millipore), monoclonal anti-glial fibrillary acidic protein (GFAP, G3893, Sigma). Fluorescently-conjugated secondary antibodies were from Molecular Probes (Invitrogen). Cells were fixed with 4% paraformaldehyde (PFA)/20% sucrose in phosphate buffered saline (PBS) for 15 min at room temperature (RT) and permeabilized with 0.1% Triton X100 in PBS for 5 min at RT. Samples were blocked for 30 min in IF buffer (2% BSA, 10% goat serum in PBS). Primary and secondary antibodies were diluted in IF buffer and incubated for 45 min at RT. Images were acquired at an upright Leica TCS SP5 AOBS TANDEM confocal microscope equipped with a 40X/0.80 APO L W UVI objective. Images were visualized and processed by using the Leica LAS AF, ImageJ and Adobe Photoshop CS3 softwares.

Viability Assay: Cells were incubated for 3 min at RT in extracellular medium (EM) (NaCl 135 mM, KCl 5.4 mM, $MgCl_2$ 1 mM, $CaCl_2$ 1.8 mM, glucose 10 mM, Hepes 5 mM, pH 7.4) containing 15 μg/mL fluoresceine diacetate (FDA), 5 mg/mL propidium iodide (PI), and 3.3 μg/mL Hoechst-33342. After incubation, cells were washed once in EM and immediately imaged. The hardware configuration for the imaging experiments was based on a Nikon FN1 upright microscope (Nikon Instruments, Prato Calenzano, Italy) equipped with an epifluorescence attachment and an electron multiplied ORCA-R2 CCD Camera (Hamamatsu Italia). Cells were imaged sequentially with DAPI (ex350/50, em460/50, to detect Hoechst), EGFP (ex480/30, em 535/40, to detect FDA fluorescence), TRITC (ex540/25, em605/55, to detect PI fluorescence) and BrightField (em HP420) filters, with a 16X objective (NIKON CFI75 LWD 16X Water 0.80 N.A. W.D. 3.0 mm). For every sample, at least 5 different fields of view were acquired. FDA staining was used as a marker of cell-membrane integrity and culture viability. For each field, the ratio of PI-positive (apoptotic) nuclei over the total number of nuclei, identified by Hoechst fluorescence, was calculated. Images were analyzed by using the Image J software.

Electrophysiological Recordings: Spontaneous postsynaptic currents were recorded in the whole cell configuration of the patch-clamp technique from neuronal cultures at DIV 14. The external recording solution contained (in mM): 145 NaCl, 2 KCl, 2 $CaCl_2$, 2 $MgCl_2$, 10 glucose, and 10 HEPES, pH 7.4. Patch pipettes, pulled from borosilicate glass capillaries (Hilgenberg, Malsfeld, Germany), had a 4 to 5 MΩ resistance when filled with intracellular recording solution containing (in mM): 150 KCl, 1 $CaCl_2$, 2 $MgCl_2$, 1 EGTA, 10 HEPES, and 2 Na_2ATP (300 mOsm and pH 7.2 with KOH). Whole cell recordings were acquired at RT with a 700B Axopatch amplifier (Molecular Devices, Sunnyvale, CA) using Clampex 10.0 software (Molecular Devices, Sunnyvale, CA). Voltage-clamp recordings were sampled at 10 kHz and digitally filtered at 3 kHz. Current clamp recordings were sampled at 10 kHz. sIPSCs or sEPSCs were recorded at RT from a holding potential of -60 mV in the presence kynurenic acid (1 mM) or Bicuculline (30 μM), respectively. At the end of each experiment, bicuculline (10 μM) or 2,3-dihydroxy-6-nitro-7-sulfamoyl-benzo(F)quinoxaline (NBQX) (20 μM) was added to confirm that synaptic events were $GABA_A$R- or AMPAR-mediated, respectively. The stability of the patch was checked by repetitively monitoring the input and series resistance during the experiments. Cells exhibiting 10–15% changes were excluded from the analysis. IPSCs and EPSCs were analysed with the Clampfit 10.0 detection module (Molecular Devices, Sunnyvale CA, USA) that exploits a sliding template-based algorithm. The threshold for IPSCs and EPSCs detections was set at 5 times the SD of the baseline noise.

For each IPSCs and EPSCs recording, averaged traces are obtained from at least 50 synaptic events. The decaying phase of GABAergic IPSCs was fitted with a biexponential function in the form:

$$y(t) = A_1 \exp(-t/\tau_1) + A_2 \exp(-t/\tau_2)$$

where A_1 and A_2 are the fractions of the respective components.

EPSCs decay time course was fitted monoexponentially according to:

$$y(t) = A\exp(-t/\tau)$$

The averaged decay time constant was calculated as follows: $\tau_{mean} = A_1\tau_1 + A_2\tau_2$. Action potentials were evoked in the current clamp mode by injecting depolarizing pulses (300–500 ms) of 0.5 nA through the recording pipette. The action potential threshold was measured by using the second derivative method.

Ca^{2+} Imaging: Cells were incubated for 20 min at RT in EM (see above) containing 1 μg/mL Fluo4-AM (F14201, Invitrogen), from a 1 mg/mL stock in pluronic F-127 20% solution/DMSO (P-3000MP, Invitrogen). After incubation, cells were washed once in EM, and immediately imaged. The hardware configuration for the imaging experiments was the same described above. Spontaneous activity in Fluo-4 loaded cultures at DIV14 was monitored for 6 min by recording fluorescence oscillations, with the EGFP filter cube and a 40X objective (NIKONCFI60 40X Water, N.A. 0.8, W.D. 3.0 IR). Excitation intensity was adjusted to minimize photobleaching and phototoxicity. The exposure time adopted in the different trials allowed for a frame rate of about 10 fps for a 650 × 512 image format. Data analysis was performed considering the changes in the fluorescence signal emitted from specific regions of interest over time were analyzed: after the correction for the background contribution and the initial fluorescence level (F_0), movies and plots showing the relative fluorescence change ($(F\text{-}F_0)/F_0$) were generated from the raw data.

Statistical Analysis: Data are shown as means ± standard error of the mean. All statistical tests were performed using a commercial package [Sigmastat, Systat Software Inc]. Based on the outcome of the Shapiro-Wilk normality test, data were analyzed by either the two-tailed unpaired Student's t-test or the Mann-Whitney U test.

Supporting Information

Supporting Information is available from the Wiley Online Library or from the author.

Acknowledgements

The authors thank M. Malerba for stereo microscope image of the drop on NSH devices; F. Succol and M. Nanni for the cell cultures; A. Scarpellini for SEM micrographs of SH devices; M. Orlando for

SEM neuron-astrocyte co-culture preparation. This research is supported by the Single Molecule Activation and Computing (FOCUS) project (Grant agreement no: 270483) funded under 7th FWP (Seventh Framework Programme); research area ICT-2009.8.7 Molecular Scale Devices and Systems.

[1] M. Lampin, R. Warocquier-Clérout, C. Legris, M. Degrange, M. F. Sigot-Luizard, *J. Biomed. Mater. Res.* **1997**, *36*, 99.
[2] D. S. Salloum, S. G. Olenych, T. C. S. Keller, J. B. Schlenoff, *Biomacromolecules* **2004**, *6*, 161.
[3] D. Falconnet, G. Csucs, H. Michelle Grandin, M. Textor, *Biomaterials* **2006**, *27*, 3044.
[4] R. G. Flemming, C. J. Murphy, G. A. Abrams, S. L. Goodman, P. F. Nealey, *Biomaterials* **1999**, *20*, 573.
[5] D. P. Dowling, I. S. Miller, M. Ardhaoui, W. M. Gallagher, *J. Biomater. Appl.* **2011**, *26*, 327.
[6] M. Kwiat, R. Elnathan, A. Pevzner, A. Peretz, B. Barak, H. Peretz, T. Ducobni, D. Stein, L. Mittelman, U. Ashery, F. Patolsky, *ACS Appl. Mater. Interfaces* **2012**, *4*, 3542.
[7] P. Clark, P. Connolly, A. S. Curtis, J. A. Dow, C. D. Wilkinson, *Development* **1990**, *108*, 635.
[8] D. Cojoc, F. Difato, E. Ferrari, R. B. Shahapure, J. Laishram, M. Righi, E. M. Di Fabrizio, V. Torre, *PLoS One* **2007**, *2*, e1072.
[9] A. Curtis, C. Wilkinson, *Biomaterials* **1997**, *18*, 1573.
[10] R. Barbucci, A. Magnani, A. Chiumiento, D. Pasqui, I. Cangioli, S. Lamponi, *Biomacromolecules* **2005**, *6*, 638.
[11] F. Bradke, C. G. Dotti, *Curr. Opin. Neurobiol.* **2000**, *10*, 574.
[12] N. Li, A. Folch, *Exp. Cell. Res.* **2005**, *311*, 307.
[13] A. A. Oliva, C. D. James, C. E. Kingman, H. G. Craighead, G. A. Banker, *Neurochem. Res.* **2003**, *28*, 1639.
[14] A. K. Vogt, G. J. Brewer, A. Offenhausser, *Tissue Eng.* **2005**, *11*, 1757.
[15] N. M. Dowell-Mesfin, M. A. Abdul-Karim, A. M. P. Turner, S. Schanz, H. G. Craighead, B. Roysam, J. N. Turner, W. Shain, *J. Neural Eng.* **2004**, *1*, 78.
[16] A. Rajnicek, S. Britland, C. McCaig, *J. Cell Sci.* **1997**, *110*, 2905.
[17] F. Haq, V. Anandan, C. Keith, G. Zhang, *Int. J. Nanomed.* **2007**, *2*, 107.
[18] A. M. P. Turner, N. Dowell, S. W. P. Turner, L. Kam, M. Isaacson, J. N. Turner, H. G. Craighead, W. Shain, *J. Biomed. Mater. Res.* **2000**, *51*, 430.
[19] J. S. Goldner, J. M. Bruder, G. Li, D. Gazzola, D. Hoffman-Kim, *Biomaterials* **2006**, *27*, 460.
[20] J. Y. Shiu, W. T. Whang, P. Chen, *J. Adhes. Sci. Technol.* **2008**, *22*, 1883.
[21] Z. Guo, F. Zhou, J. Hao, W. Liu, *J. Am. Chem. Soc.* **2005**, *127*, 15670.
[22] X. J. Feng, L. Jiang, *Adv. Mater.* **2006**, *18*, 3063.
[23] D. J. Fabrizius-Homan, S. L. Cooper, *J. Biomed. Mater. Res.* **1991**, *25*, 953.
[24] C. J. Wilson, D. I. Leavesley, M. J. Pearcy, *Tissue Eng.* **2005**, *11*, 17.
[25] T. L. Sun, L. Feng, X. F. Gao, L. Jiang, *Accounts. Chem. Res.* **2005**, *38*, 644.
[26] N. E. Paula, C. Skazik, M. Harwardt, M. Bartneck, B. Denecke, D. Klee, J. Salber, G. Zwadlo-Klarwasser, *Biomaterials* **2008**, *29*, 4056.
[27] A. B. D. Cassie, S. Baxter, *Trans. Faraday Soc.* **1944**, *40*, 546.
[28] S. Kaech, G. Banker, *Nat. Protoc.* **2006**, *1*, 2406.
[29] M. Caiazzo, M. T. Dell'Anno, E. Dvoretskova, D. Lazarevic, S. Taverna, D. Leo, T. D. Sotnikova, A. Menegon, P. Roncaglia, G. Colciago, G. Russo, P. Carninci, G. Pezzoli, R. R. Gainetdinov, S. Gustincich, A. Dityatev, V. Broccoli, *Nature* **2011**, *476*, 224.
[30] M. E. Schwab, *Curr. Opin. Neurobiol.* **2004**, *14*, 118.
[31] F. De Angelis, F. Gentile, F. Mecarini, G. Das, M. Moretti, P. Candeloro, M. L. Coluccio, G. Cojoc, A. Accardo, C. Liberale, R. P. Zaccaria, G. Perozziello, L. Tirinato, A. Toma, G. Cuda, R. Cingolani, E. Di Fabrizio, *Nat. Photonics* **2011**, *5*, 682.

Received: June 20, 2012
Revised: August 10, 2012
Published online: October 2, 2012